Laser control of photopredissociation angular distributions and photoionization in Cl2 by two color interference

André D. Bandrauk, JeanMarc Gauthier, and James F. McCann

Citation: The Journal of Chemical Physics **100**, 340 (1994); doi: 10.1063/1.466947
View online: http://dx.doi.org/10.1063/1.466947
View Table of Contents: http://scitation.aip.org/content/aip/journal/jcp/100/1?ver=pdfcov
Published by the AIP Publishing

Laser control of photopredissociation angular distributions and photoionization in Cl_2 by two color interference

André D. Bandrauk and Jean-Marc Gauthier
Laboratoire de Chimie Théorique, Faculté des Sciences, Université de Sherbrooke, Sherbrooke, Quebec J1K 2R1, Canada

James F. McCann
Physics Department, University of Durham, Durham DH1 3LE, United Kingdom

(Received 28 June 1993; accepted 15 September 1993)

A coupled equations approach based on a general artificial channel method is used to demonstrate two color laser coherent control of photopredissociation and photoionization in Cl_2. Photopredissociation of the $^1\Pi_g$ states of Cl_2 is suppressed by a two plus four photon interference process $2\omega_2=4\omega_4$, whereas the photoionization is controlled by interference between a six photon transition and a four photon transition $6\omega_4=2\omega_2+2\omega_4$ using the same $^1\Pi_g$ photopredissociation resonances as intermediates. Photopredissociation angular distributions illustrate the suppression of the corresponding transition in selective rotational states.

INTRODUCTION

Controlling photochemical processes using coherent laser sources is now becoming an area of research attracting the attention of an increasing number of photochemists and chemical physicists. It is an area where theory has been very much in the forefront, exploring various control scenarios by simulation. Some approaches are based on the exploitation of quantum interference effects,[1–3] whereas other scenarios rely on the coherence inherent in multiphoton transitions at high intensities.[4–7] In all cases, phase and amplitude of the exciting laser fields are the essential control parameters (see Ref. 8 for more details).

In the present work, we will focus on simulation of the control of predissociation angular distributions in the Π_g states of Cl_2 via two color interference of the photoexcitation pathways from the ground $X\,^1\Sigma_g^+$ to the excited $^1\Pi_g$ states. The control is achieved by varying the relative phase of the two color sources. Thus previous suggested scenarios were based on interference between one and three photon pathways.[2] Experimental verification of this latter scheme has been achieved recently in controlling ionization of atoms[9] and molecules.[10] We have recently proposed that two and four photon interferences should be useful in controlling photochemical or photophysical processes such as predissociation in states with the same symmetry as the ground state.[11] The present calculation is an extension of the above preliminary work, which reported only control of predissociation rates. We will show that photopredissociation angular distributions can be also controlled at will due to the suppression of predissociation of a selective rovibrational level by simultaneously interfering the two and four photon excitation pathways with different relative phases of one of the incident radiation fields. In addition, we have added an ionization channel to show that photopredissociation and photoionization can be controlled independently.

The present numerical study relies only on known electronic surfaces and transition moments of the Cl_2 molecule. These data can be either obtained from *ab initio* quantum calculations[12,13] or from spectroscopic measurements.[14] Thus given electronic potentials and transition moments, cw laser induced transition *amplitudes* can be calculated exactly using a generalized artificial channel method.[15,16] We emphasize that the numerical method used here calculates amplitudes rather than transition probabilities, thus making the method very useful for simulating interference phenomena which involve interfering amplitudes with different phases.

COUPLED EQUATIONS AND ARTIFICIAL CHANNEL METHOD

We wish to model the interference between the two (frequency ω_2) and four (frequency ω_4) photon transition amplitudes from the ground $X\,^1\Sigma_g^+$ state to the predissociative $^1\Pi_g$ state (Fig. 1). Such a two color problem can be treated formally and numerically using field–molecule or *dressed* states.[15–17]

The total wave function is therefore defined as

$$\psi_j(R,r)=\langle R,r|j\rangle=R^{-1}F_j(R)\theta_j(\hat{R})\phi_j(R,r)\,|n_j\rangle, \qquad (1)$$

where R and r represent nuclear and electronic coordinates, respectively. F_j is a nuclear radial function, θ_j is a rotational function, ϕ_j is an electronic wave function, and $|n_j\rangle$ is a quantized field eigenstate. The j subscript is a shorthand notation for the ensemble of electronic, nuclear, and photon quantum numbers $\{\Lambda_j J_j M_j,\ v_j \text{ or } k_j\}$ with v_j a vibrational nuclear quantum number and k_j a nuclear wave number.

The dressed energies or potentials are defined as eigenergies of the uncoupled field (H_f) and molecule (H_m) Hamiltonians

 0021-9606/94/100(1)/340/10/$6.00

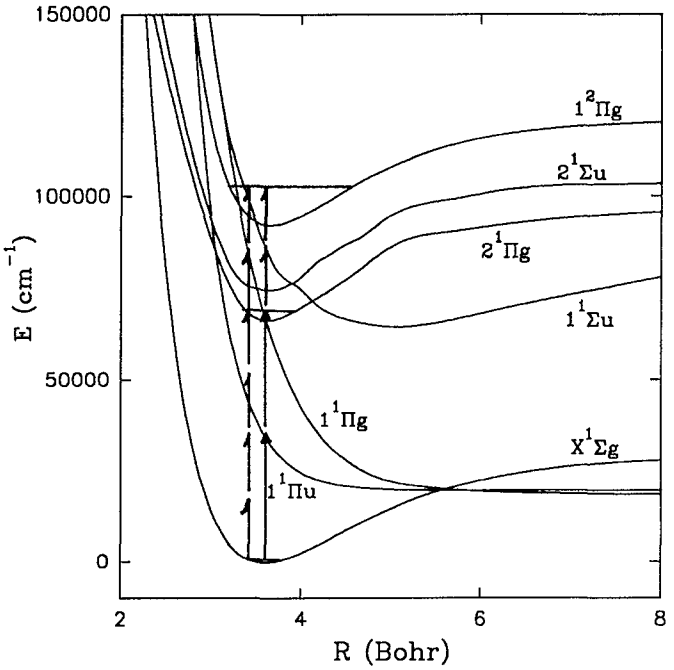

FIG. 1. Diabatic potentials of Cl_2 and Cl_2^+ showing interfering ω_2 photon ($\rightarrow$) and ω_4 photon ($\rightarrow$) processes.

$$(H_f+H_m)\psi_j(R,r)=E_j\psi_j(R,r) \tag{2}$$

with

$$E_j=\epsilon_j(R)+\sum_{k=1}^{2}\hbar\omega_{2k}n_{j,2k}, \tag{3}$$

where $\epsilon_j(R)$ is the total molecular energy of channel j and the last term is the total photon energy for the photon numbers $n_{j,2k}$ of frequencies ω_2 and ω_4 such that $2\omega_4=\omega_2$.

The total Hamiltonian is written as

$$H=H_m+H_{\rm nd}+H_f+H_{mf}, \tag{4}$$

where

$$H_f=\sum_{k=1}^{2}\hbar\omega_{2k}a_{2k}^{+}a_{2k}, \tag{5}$$

so that

$$H_f|n_j\rangle=\sum_{k=1}^{2}\hbar\omega_{2k}n_{j_{2k}}|n_j\rangle \tag{6}$$

and

$$|n_j\rangle=|n_{j,2}\rangle\,|n_{j,4}\rangle.$$

This allows us to define the radiative molecule coupling as

$$H_{mf}=\sum_{k=1}^{2}\left(\frac{\hbar\omega_{2k}}{2V}\right)^{1/2}\epsilon^{(2k)}\cdot d(a_{2k}^{+}+a_{2k}), \tag{7}$$

where d is the electronic transition moment and ϵ is the polarization vector. We choose in the present control scenario linearly polarized radiation only.

Furthermore, in Eq. (4), we encounter nonradiative couplings. In the particular case we are examining, the two Π_g states $1\,^1\Pi_g$ and $2\,^1\Pi_g$ are coupled nonadiabatically by corrections due to the breakdown of the Born–Oppenheimer approximation, leading to predissociation.[18,19] One can choose a *diabatic* representation, corresponding to well-defined single electronic configurations, for which the electronic part of H_m, i.e., $H_{\rm el}$, is nondiagonal

$$H_{\rm el}(r,R)\phi_j^d(r,R)=V_j(R)\phi_j^d(r,R), \tag{8}$$

$$\langle j|H_{\rm nd}|j'\rangle=\langle\phi_j^d|H_{\rm el}|\phi_{j'}^d\rangle=V_{jj'}(R). \tag{9}$$

In this case, the two electronic $^1\Pi_g$ potentials cross (see Fig. 1) and the two diabatic electronic states are coupled by a nondiabatic potential term $V_{jj'}(R)$ [Eq. (9)]. The diabatic potentials V_j and nondiabatic couplings $V_{jj'}(R)$ for the two $^1\Pi_g$ states in Fig. 1 have been obtained from the *ab initio* adiabatic $^1\Pi_g$ potentials[12,13] by a standard deperturbation procedure.[15] This also leads to diabatic transition moments which serve as input in the coupled equations method described below.

For an m photon absorption followed by a nonradiative transition to a final continuum state, the total transition amplitude can be defined in leading-order perturbation theory as

$$T_{fi}(E,\hat{k})=\sum_{j_1,\cdots j_m}\frac{\langle f|H_{\rm nd}|j_m\rangle\langle j_m|H_{mf}|j_{m-1}\rangle\cdots\langle j_1|H_{mf}|i\rangle}{(E-E_m)(E-E_{m-1})\cdots(E-E_1)}, \tag{10}$$

where the initial $|i\rangle$ state is a bound state and the final state $|f\rangle$ is a continuum state (Fig. 1). Thus the multiphoton-assisted dissociation probability per unit time w_{fi} is obtained from

$$dw_{fi}(E,\hat{k})=\frac{2\pi}{\hbar}\,|T_{fi}(E,\hat{k})|^2 d\rho_f, \tag{11}$$

where ρ_f is the density of final continuum states, $\hat{k}$ is the direction of fragments, and E is the total (conserved) field–molecule energy. T is the total transition matrix from the initial bound to final continuum states. The matrix elements in Eq. (10) involve integrals over all internal coordinates (r,R and spins). The summations involve complete sets of intermediate states, resonant and nonresonant.

Two computational difficulties arise in performing these summations correctly. First, continuum states are infinite in number in addition to creating singularities in the energy denominators in the sums in Eq. (10). Second, in the present case, the two $^1\Pi_g$ states are strongly coupled, so that the first order nonradiative nondiabatic matrix element $\langle f|H_{nd}|j_m\rangle$ does not suffice to correctly describe the nondiabatic couplings. We thus have a situation where the radiative matrix elements are perturbative, but involve many bound–continuum transitions, whereas the nondiabatic couplings are nonperturbative and also involve bound–continuum transitions. In the past, we have shown that multiphoton transitions in the presence of nondiabatic (nonradiative) interactions can be treated consistently from the weak interaction, perturbative limit to the strong, nonperturbative limit for both radiative and nonradiative transitions by coupled equations methods using artificial channel methods.[15–17]

The dressed state representation allows one to write the total Schrödinger equation $H\psi=E\psi$ as coupled second-order differential equations[15–17]

$$\left[-\frac{\hbar^2}{2m}\frac{d^2}{dR^2}+V_j^n(R)-E\right]F_j^n(R)=\sum_{j'}V_{jj'}^{n'}(R)F_{j'}^{n'}(R), \tag{12}$$

where the F's are the nuclear, bound (vibrational), or continuum (dissociative), radial functions. The field–molecule potentials are defined from Eq. (3) as [they include rotational energies $\hbar^2J_j(J_j+1)/2mR^2$]

$$V_j^n(R)=V_j(R)+n_{j,2}\hbar\omega_2+n_{j,4}\hbar\omega_4, \tag{13}$$

whereas the off-diagonal couplings are of two types—radiative and nonradiative. The radiative couplings can be written as a *Rabi* frequency ω_R,

$$\begin{aligned}\frac{\hbar\omega_R}{2}&=V_{jj'}^{n'}(\mathrm{cm}^{-1})\\&=d_{jj'}(R)\mathscr{E}_0\delta_{n',n\pm1}/2\\&=5.85\times10^{-4}d_{jj'}(\mathrm{a.u.})[I(\mathrm{W/cm}^2)]^{1/2},\end{aligned} \tag{14}$$

where $I=(c\mathscr{E}_0^2)/(8\pi)$ defines the relation between the field intensity I and the amplitude $\mathscr{E}_0$. The nondiabatic (nonradiative) coupling H_{nd} has been defined in Eq. (9) and is diagonal in photon number n.

Since the initial state is a bound state and the final state is a continuum state, one would like to convert the whole problem into a scattering problem, thus enabling one to treat bound and continuum states and their interactions exactly. This is achieved by adding an additional continuum $|c\rangle$, called the *artificial* channel, coupled weakly, i.e., perturbatively to the initial state $|i\rangle$. Calculation of the transition amplitude T_{cf} between artificial $|c\rangle$ and final $|f\rangle$ continuum states allows one to extract exact transition amplitudes T_{if}.[15–17,20]

The coupled differential equations (12) can be written formally as

$$(L-V)F=0, \tag{15}$$

where

$$L_{ij}=\delta_{ij}\left[\frac{d^2}{dR^2}+k_j^2(E,R)\right], \tag{16}$$

$$k_j^2(E,R)=\frac{2m}{\hbar^2}[E-V_j^n(R)]. \tag{17}$$

Within each electronic manifold, we take account of all rotational levels by adding the rotational energies $\hbar^2J_j(J_j+1)/2mR^2$. The probability amplitudes of the rotational states determine the angular distribution of the dissociation products. The radiative couplings in Eqs. (12) and (14) will involve vector-coupling coefficients or Wigner 3-j symbols[21] appropriate for different electronic transitions. Thus for $^1\Sigma$–$^1\Pi$ and $^1\Pi$–$^1\Pi$ transitions considered here, these have been given previously in our papers on laser induced alignment in multiphoton dissociation of diatomics.[17]

The set of Eq. (12) or Eq. (15) is supplemented by those involving artificial continuum channels. The method originally introduced by Shapiro to treat perturbative direct one photon photodissociation[22] has been extended to the calculation of multiphoton transitions.[15–17] Introduction of artificial bound channels has been successful in treating intense field Raman processes[23] and intense field photodissociation.[20] In the present case, one needs to couple the initial state $|i\rangle$ only to one artificial continuum channel $|c\rangle$ to act as the entrance channel for a scattering wave. The total Hamiltonian (4) is consequently modified by the addition of the artificial coupling term

$$H_{ic}=\left(\frac{\hbar\Gamma_i}{2\pi}\right)^{1/2}(|i\rangle\langle c|+|c\rangle\langle i|), \tag{18}$$

where the artificial channel induced width Γ_i of the state $|i\rangle$ is determined *a priori* by means of a preliminary calculation involving only the two channels $|i\rangle$ and $|c\rangle$ based on an isolated (perturbative) resonance S-matrix calculation. The complete set of coupled differential equations (15) is then integrated numerically using a Fox–Goodwin algorithm, a modification of the Numerov method, as originally described by Norcross and Seaton.[24] The quadrature begins at the origin and is integrated outwards, subject to the boundary conditions for incoming flux in channel $|i\rangle$,

$$F_j(J_j,0)=0$$

and outgoing asymptotic forms

$$F_j(J_j,R)_{R\to\infty}\sim\begin{cases}[\delta_{ij}\exp(-ik_jR+iJ_j\pi/2)-S_{ij}\exp(ik_jR-iJ_j\pi/2)], & k_j^2>0,\\ [-S_{ij}\exp(-|k_j|R-iJ_j\pi/2)], & k_j^2<0.\end{cases} \tag{19}$$

The corresponding transition matrix T_{if} is defined by the relation

$$S_{if}=\exp(i\eta_i+i\eta_f)(\delta_{if}-2\pi i T_{if}), \tag{20}$$

where $\eta_{i(f)}$ represents the elastic phase shifts. The numerical integration procedure thus supplies the S or equivalently T matrix for the open channels. The differential equations (12) and (15) can be rewritten as an equivalent integral equation for the T matrix.[15–17]

$$T(E)=V+VL^{-1}(E)T(E), \tag{21}$$

from which it follows that

$$T_{cf}(E)=V_{ci}L_{ii}^{-1}(E)T_{if}(E). \tag{22}$$

T_{cf} represents the transition amplitude from the artificial continuum $|c\rangle$ to the final continuum state $|f\rangle$. Using the weak coupling or equivalently isolated resonance expression for the initial state Green's function L_{ii}^{-1},

$$L_{ii}^{-1}(E)=(E-E_i-\Delta_i+i\Gamma_i/2)^{-1}, \tag{23}$$

where Δ_i the level shift and $\Gamma_i=[(2\pi)/\hbar]|V_{ci}|^2$ the level width are determined from a preliminary two channel resonance calculation, then on resonance ($E=E_i+\Delta_i$), one obtains the numerical photopredissociation transition amplitudes of interest $T_{if}^{\rm pd}$,

$$T_{if}^{\rm pd}(E)=i\left(\frac{\pi}{2\Gamma_i}\right)^{1/2}\cdot T_{cf}(E). \tag{24}$$

The total dissociation rate per unit solid angle $w(E,\hat{k})$ [Eq. (11)] from the initial state $|i\rangle$ to the final state $|f\rangle$ in the direction $\hat{k}$ at total energy E is given by

$$w(E,\hat{k})=4\pi^2\hbar k_f m^{-1}\Big|\sum_f \exp(-i\pi J_f/2)\theta_f(\hat{k})T_{if}^{\rm pd}\Big|^2. \tag{25}$$

$T_{if}^{\rm pd}$ is made up of two different amplitudes—the two photon amplitude $T_2(\omega_2)$ corresponding to photodissociation via photons ω_2 and the four photon amplitude $T_4(\omega_4)$ from excitation by photons of frequency ω_4. These two independent amplitudes can have a relative phase ϵ which is controlled by the laser conditions (see the next section), i.e., the total transition amplitude can be written as

$$T^{\rm pd}=T_2(\omega_2)\exp(i\epsilon)+T_4(\omega_4). \tag{26}$$

Cancellation in the total photopredissociation transition amplitude $T_{if}^{\rm pd}$ or probability $|T_{if}^{\rm pd}|^2$ will therefore occur whenever $|T_2|=|T_4|$ and $\arg(T_2)+\epsilon-\arg(T_4)-\pi=0$. Cancellations of photopredissociation yields from the ground $X\,^1\Sigma_g^+$ to the $^1\Pi_g$ states were reported earlier[9] and were found to occur selectively, i.e., for each individual $^1\Pi_g$ vibrational level, different phases and laser intensities were required to suppress predissociation of these states. In the next section, we will explore variations of photopredissociation angular distributions as a function of the relative phase ϵ of the two laser fields $\mathscr{E}(\omega_2)$ and $\mathscr{E}(\omega_4)$ with intensities I_2 and I_4.

We will also include ionization of the Cl_2 molecule since the four photon transition which is nonresonant between the $X\,^1\Sigma_g^+$ and $^1\Pi_g$ states approaches the ionization threshold intensities [$I(\omega_4)\sim 10^{10}$ W/cm^2].[14] This will allow us to examine the relative control efficiency of ionization and photopredissociation and the competition between these processes. Thus as shown in Fig. 1, a fifth photon of frequency ω_4 couples radiatively the diabatic $^1\Pi_g$ states to the diabatic $^1\Sigma_u^+$ states and a sixth photon induces a final transition to the $^2\Pi_g$ vibrational levels of Cl_2^+. An effective transition moment (see the next section) is used to describe this last transition which involves an electronic transition from a bound molecular orbital to a continuum electron orbital. Thus Fig. 1 corresponds to a zero-kinetic energy (ZEKE) electron, i.e., the total final energy is that of a final $^2\Pi_g$ vibrational energy level of Cl_2^+ illustrated in that figure. The actual calculation is now performed by adding a second artificial continuum channel $|c'\rangle$ coupled weakly to the $^2\Pi_g$ potential, so that the total artificial channel transition amplitude $T_{cc'}$ becomes

$$T_{cc'}=V_{ci}L_{ii}^{-1}T_{if}^{\rm pi}L_{ff}^{-1}V_{fc'}, \tag{27}$$

from which at resonance $E=E_i+\Delta_i=E_f+\Delta_f$, one obtains the photoionization amplitude

$$T_{if}^{\rm pi}=\pi/2(\Gamma_i\Gamma_f)^{-1/2}T_{cc'}. \tag{28}$$

Γ_i and Γ_f are the artificially induced small widths of the initial ground rovibrational level ($X\,^1\Sigma_g^+$) of Cl_2 and of the final rovibrational level ($^2\Pi_g$) of Cl_2^+, respectively. These are obtained from separate two channel resonance S-matrix calculations as indicated above.

Again two different pathways are possible in photoionization. A direct six photon photoionization with amplitude $T_6(\omega_4)$ induced by photons of frequency ω_4 or alternatively a four photon transition induced by two photons of frequency ω_2 and two photons of frequency ω_4 (see Fig. 1). This last amplitude can be written as

$$T_4(\omega_2,\omega_4)=T_2(\omega_2)G(^1\Pi_g)T_2(\omega_4), \tag{29}$$

where $G=(E-H_m-H_f-H_{\rm nd})^{-1}$ is the molecule–field Green's function for the intermediate $^1\Pi_g$ states of Cl_2 including the nondiabatic interaction $H_{\rm nd}$. The total transition amplitude for photoionization including the effect of the relative laser field phase ϵ is now written as

$$T^{\rm pi}=T_4(\omega_2,\omega_4)\exp(i\epsilon)+T_6(\omega_4). \tag{30}$$

Cancellation or enhancement of $T^{\rm pi}$ is thus to be expected again as ϵ the relative phase between both incident laser fields is varied.

In summary, the artificial channel method allows one to obtain both the bound $(v_i,J_i,X\,^1\Sigma_g^+)$ to continuum $(k_f,J_f,1\,^1\Pi_g)$ *photopredissociation* amplitude $T_{if}^{\rm pd}$ of Cl_2 via Eq. (24). Simultaneously, one can obtain the *photoionization* amplitude $T_{if}^{\rm pi}$ for the transition from the initial bound state above $(v_i,J_i,X\,^1\Sigma_g^+)$ of Cl_2 to some final rovibrational level $(v_f,J_f,1\,^2\Pi_g)$ of Cl_2^+ via Eq. (28). Thus Eq. (24) gives the photopredissociation probabilities $|T_{if}^{\rm pd}|^2$ and the corresponding angular distribution follows from Eq. (25). The photoionization probability is obtained from $|T_{if}^{\rm pi}|^2$ with $T_{if}^{\rm pi}$ calculated from Eq. (28). We have used such a procedure before in a numerical study of the ten-photon ionization of H_2 in intense laser fields.[25]

TRANSITION AMPLITUDES

In the previous section, we have shown in detail how one can obtain from a numerical S-matrix calculation, the exact transition amplitudes for photopredissociation T_{if}^{pd} and photoionization T_{if}^{pi} by introducing an artificial continuum $|c\rangle$ coupled to the initial $|X\,^1\Sigma_g^+, v_i, J_i\rangle$ state. Thus in the case of photopredissociation, the final state becomes a continuum state $|1\,^1\Pi_g, k_f, J_f\rangle$, whereas for photoionization, an extra artificial channel $|c'\rangle$ is needed as exit channel from some bound rovibrational level of Cl_2^+, $|^2\Pi_g, v_f, J_f\rangle$. The input data into the coupled equation (12) or Eq. (16) are radiative transition moments $V_{jj'}^{n'}$, [Eq. (14)] nonradiative nondiabatic couplings between the $^1\Pi_g$ states and $^1\Sigma_u^+$ states of Cl_2, $V_{jj'}(R)$ [Eq. (9)]. These data have been tabulated in our previous study of nonadiabatic multiphoton effects in Cl_2.[15] We summarize briefly some of the input data. Strong transition moments occur between the $X\,^1\Sigma_g^+$ and $2\,^1\Sigma_u^+$ states and between $1\,^1\Pi_u$ and $1\,^1\Pi_g$. Since in both cases one is dealing with single electron excitation between molecular orbitals made up of the same atomic orbitals, i.e. $(3p\sigma_a \pm 3p\sigma_b)$ and $(3p\pi_a \pm 3p\pi_b)$, then in general one expects these transition moments to behave as $R/2$.[15,25] Such a linear increase is typical of charge resonance transfer[26] and is corroborated by *ab initio* calculations.[13] The $2\,^1\Pi_g$–$2\,^1\Sigma_u^+$ transitions are of Rydberg type and can also be quite large (~ 6 a.u. in the present case). The $2\,^1\Sigma_u^+(Cl_2)$–$1\,^2\Pi_g(Cl_2^+)$ Rydberg-ionization transition moment being unknown was arbitrarily set as an effective bound–bound transition moment of 1 cm^{-1}. In the present calculation, we have considered only a single ionized electron kinetic energy, i.e., zero kinetic energy (ZEKE) corresponding to Fig. 1. In principle, one can scan all possible electron kinetic energies by shifting up continuously the $^2\Pi_g$ state as was done in the ten-photoionization calculation for H_2.[25] However, in view of the low field intensities used here $I < 10^9$ W/cm^2, ionization yields are very low and are therefore perturbative, so that only one kinetic energy channel (the ZEKE channel) is adequate in the present simulation. The nondiabatic couplings between the Rydberg ($2\,^1\Sigma_u^+$) and valence ($1\,^1\Sigma_u^+$) diabatic states was obtained from a deperturbation[15] of previous *ab initio* adiabatic potentials,[12] yielding $H_{nd}(^1\Sigma_u^+) = 946$ cm^{-1}. The nondiabatic coupling between the $^1\Pi_g$ states was obtained by fitting the resonances from a two-channel S-matrix calculation to the observed $^1\Pi_g$ levels,[14] yielding a value $H_{nd}(\Pi_g) = 350$ cm^{-1}. Such a value of nondiabatic coupling between the diabatic $1\,^1\Pi_u$ and $2\,^1\Pi_u$ is considered to be of intermediate coupling strength and cannot be treated perturbatively.[18] The present coupled equations approach covers all regimes, perturbative and nonperturbative alike.

Finally, the fields which enter the radiative couplings [Eq. (14)] can be expressed as

$$\mathscr{E}(t) = \mathscr{E}_0 \cos(\omega t + \epsilon/2) = \frac{\mathscr{E}_0}{2}\left[\exp\left(i\omega t + \frac{i\epsilon}{2}\right) + \exp\left(-i\omega t - \frac{i\epsilon}{2}\right)\right]. \quad (31)$$

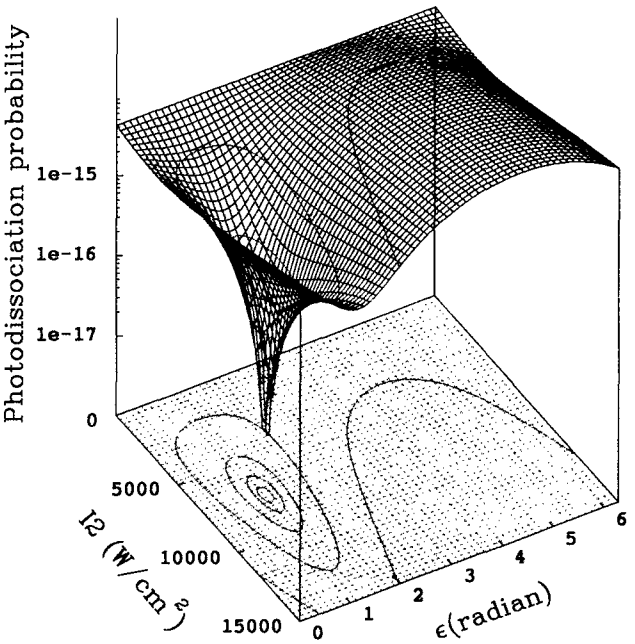

FIG. 2. Photopredissociation probability via the $v=0$, $J=2$ level of the $2\,^1\Pi_g$ state for fixed $I_4 = 5\times10^8$ W/cm^2 vs I_2 and relative phase ϵ. Minimum occurs at $I_2 = 7359$ W/cm^2 and $\epsilon = 0.37\pi$. $\omega_2 = 2\omega_4 = 33\,210$ cm^{-1}.

Retaining only one term of Eq. (31) is equivalent to applying the rotating wave approximation RWA.[8,27] Such an approximation is valid provided the Rabi frequency ω_R [Eq. (14)] is much less than the photon frequency. Thus at a maximum intensity of 10^8 W/cm^2 used here, $\omega_R \simeq 6$ cm^{-1}/a.u., well below the photon frequency ω_4(6000 Å) $= 16\,000$ cm^{-1}. Hence only one exponential of Eq. (31) need be retained $\exp(i\omega t + i\epsilon/2)$, which corresponds to including only absorption processes in the numerical dressed state calculations, i.e., transitions $\Delta n = -1$ only. This has the advantage of simplifying the phase dependent interference calculations. Thus from Eq. (14), one calculates the two photon amplitudes T_2 separately from the four photon amplitudes T_4 for fixed laser intensities I_2 and I_4. Then using Eq. (26), one can calculate the total amplitude as a function of relative phase ϵ between the two laser fields. A similar procedure is followed to calculate the interference between the different pathways in the photoionization amplitude [Eq. (30)]. One calculation at a particular phase was performed for both amplitudes by putting the phase in the radiative couplings into the coupled equations (12). Both methods gave the same results and thus served as a validation of Eqs. (26) and (30).

All calculations were performed using as an initial state $|X\,^1\Sigma_g^+, v_i=0, J_i=0\rangle$ and assuming linearly polarized light, so that the selection rule $\Delta M_J = 0$ was respected in all transitions. The laser frequencies were scanned such that $2\omega_2 = 4\omega_4$ corresponded to a resonant transition into the $^1\Pi_g$ vibrational manifold. Due to the initial state condition, only $J=1$ of the $1\,^1\Pi_u$ continuum is populated resonantly by ω_2 photons followed by a radiative transfer to

the $J=2$, $^1\Pi_g$ states. The ω_4 photon induces nonresonant transitions to $J=1$ of $^1\Sigma_u^+$; $J=2$ of $^1\Pi_g$; $J=1$, 3 of $^1\Sigma_u^+$ and finally $J=2,4$ of $^1\Pi_g$ of Cl_2. Thus only the $J=2$ rotational state of the $^1\Pi_g$ manifold can be affected by the two excitation path (ω_2 and ω_4) interference. $J=4$ states remain unaltered. Finally a fifth ω_4 photon induces resonant transitions to $J=1,3,5$, $^1\Sigma_u^+$ states from which ionization occurs to $J=2$, 4, and 6 rovibrational levels of the $^2\Pi_g$ electronic state of Cl_2^+. (We note that $J=0$ states do not exist in the $^1\Pi$ manifold and are excluded from all discussions.[19])

RESULTS

Equations (26) and (30) predict a well-known, but little exploited phenomenon—quantum mechanical interferences between amplitudes leading from a common initial state to a common final state, i.e., both transition pathways must connect a common initial state to a unique final state in order to suppress or enhance the transition. Such suppression and enhancement in the photopredissociation yields (Fig. 2) and angular distribution (Fig. 3) are observed clearly for the total two ($2\omega_2$) and four ($4\omega_4$) photon transitions to the $v=0$, $J=2$ predissociated level of the $^1\Pi_g$ electronic manifold, which is made up of two diabatic $1\,^1\Pi_g$ and $2\,^1\Pi_g$ electronic potentials coupled by a nondiabatic perturbation $H_{nd}(\Pi_g)=350\ cm^{-1}$. The suppression at conditions $\epsilon=0.37\pi$, $I_2=7359\ W/cm^2$ is total (absolute zero), whereas the enhancement at $\epsilon=1.37\pi$ is weak. The angular distribution (Fig. 3) shows the gradual evolution from a dominant $J=2$ partial wave contribution finally to a weak residual $J=4$ partial wave contribution, as the $J=2$ partial wave is eliminated by phase interference.

Of note is the possible control of the total angular distribution by interference between $J=2$ and 4 partial waves as illustrated in Fig. 4. Thus around $\epsilon=0.38\pi$, the amplitude of the $J=2$ partial wave approaches in magnitude that of the $J=4$ component (see Table I), so that destructive interference between these two partial waves can also occur. As illustrated in Fig. 4, complete suppression of photopredissociation can be achieved, whereas in Fig. 3, at $\epsilon=0.37\pi$, the photodissociation channel leads to pure $J=4$ products only.

Figure 5 illustrates the ionization yield of molecular Cl_2^+ ions in the $J=2$ state to be expected with the predissociated $v=0$ level as intermediate resonance. Suppression occurs at $\epsilon=0.54\pi$ and $I_2=3747\ cm^{-1}$ ($I_4=5\times10^8$ W/cm^2 as in Figs. 2 and 5). Clearly the suppression of the ionization occurs at conditions different from the photopredissociation (Figs. 2 and 3). This can be rationalized by the fact that nonresonant intermediate transitions play a role in the photoionization. Thus in the photopredissociation, one is controlling the yield of a single final state, the $J_f=2$ continuum state of the $1\,^1\Pi_g$ potential (see Fig. 1) via two and four photon interferences. In the photoioniza-

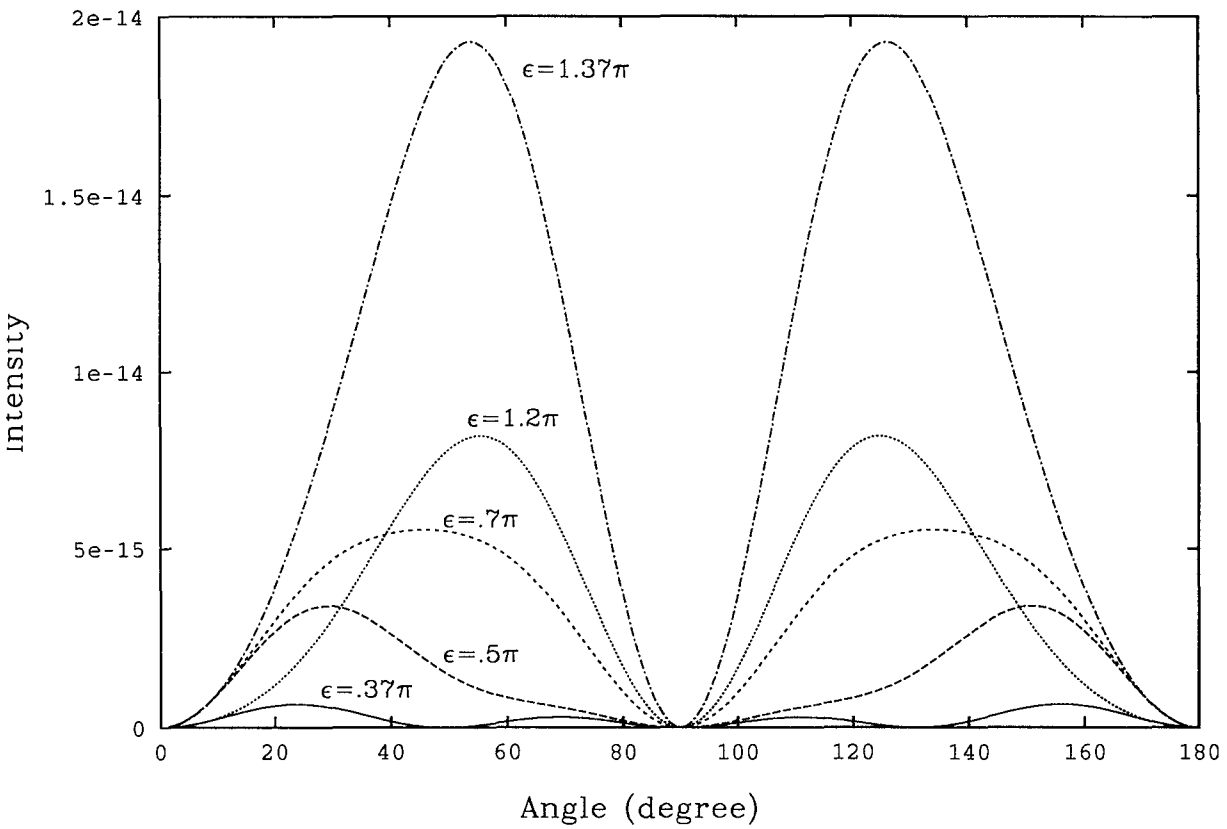

FIG. 3. Photopredissociation angular distribution for the $v=0$, $J=2$ level at the minimum of Fig. 2 $I_4=5\times10^8$ W/cm^2, $I_2=7359$ W/cm^2 vs relative phase ϵ. $\omega_2=2\omega_4=33\,210\ cm^{-1}$.

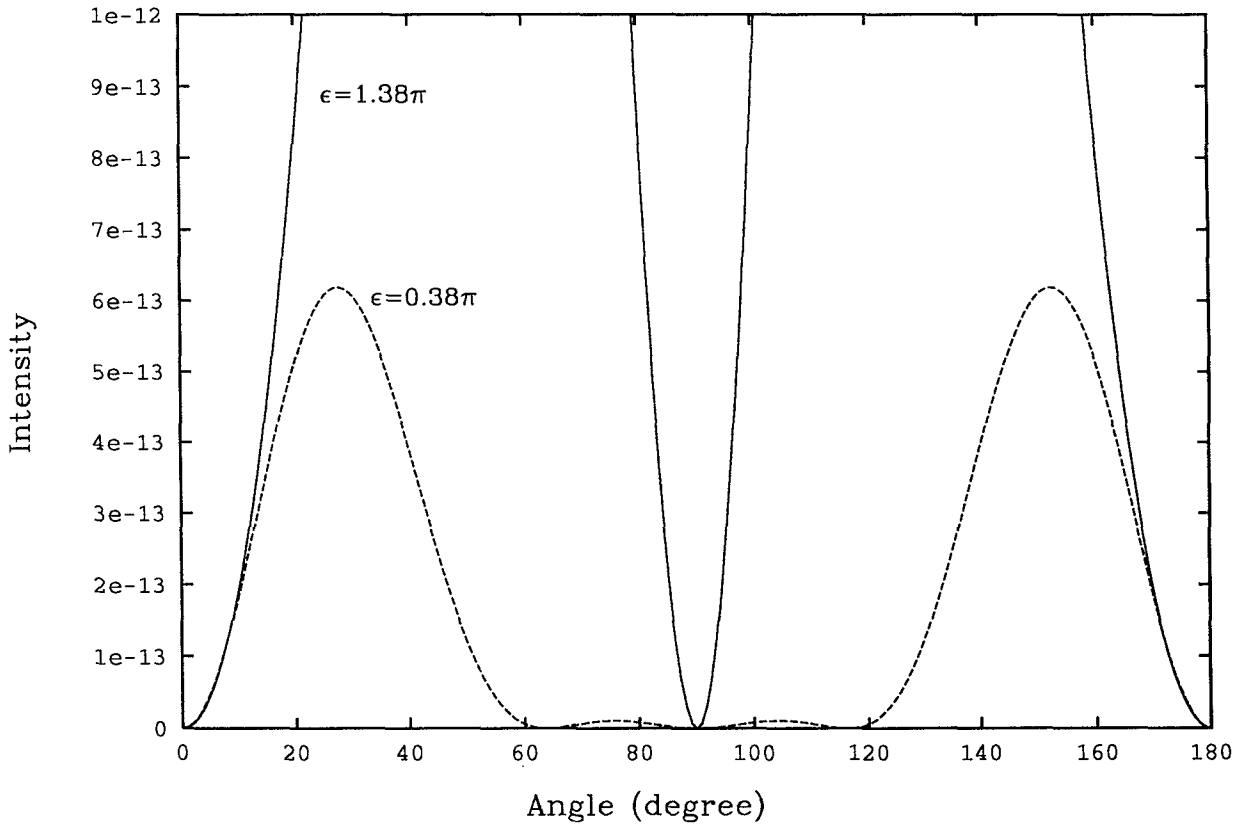

FIG. 4. Photopredissociation angular distribution at $I_4=5\times10^8$ W/cm^2, $I_2=10\,282$ W/cm^2 vs relative phase ϵ for $v=0$, showing interference between $J=2$ and 4 partial waves. $\omega_2=2\omega_4=33\,210$ cm^{-1}.

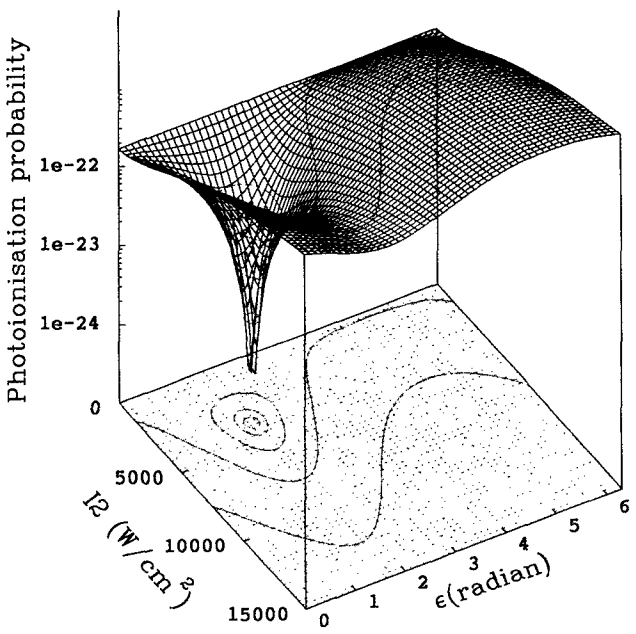

FIG. 5. Photoionization yield in partial wave $J=2$ with the $v=0$, $J=2$ level of 2 $^1\Pi_g$ as intermediate resonance for $I_4=5\times10^8$ W/cm^2 vs I_2 and relative phase ϵ. Minimum occurs at $I_2=3747$ W/cm^2, $\epsilon=0.54\pi$. $\omega_2=2\omega_4=33\,210$ cm^{-1}.

tion, resonant and nonresonant contributions from the $v_f=0$, $J_f=2$ quasibound level of the 2 $^1\Pi_g$ potential and also the $J_f=2$ continuum of the 1 $^1\Pi_g$ potential play a role. Thus the resonant amplitude would correspond to the photopredissociation amplitude, whereas the nonresonant amplitudes involve sums over many nonresonant states. This can be seen from the general expression for a continuum Green's function which occurs as a denominator in the general amplitude expression (10),[15,16] or in the composite photoionization amplitude [Eq. (30)]

$$G(E)=(E-\hat{H}+i\eta)^{-1}=\mathrm{PP}(E-\hat{H})-i\pi\delta(E-\hat{H}). \quad (32)$$
$$\lim \eta\to 0$$

PP here means a principle part integral, over all *nonresonant* states $|i\rangle$ with energy $E\neq\langle i|\hat{H}|i\rangle$, and $\delta(E-\hat{H})$ is the *resonant* contribution $E=\langle i|\hat{H}|i\rangle$. Hence referring to Eqs. (10) and (32), one sees that suppressing resonant processes leaves higher order nonresonant processes unaltered. Figures 2 and 5 illustrate therefore that nonresonant effects can make control of physically different processes, such as dissociation and ionization, quite independent. This is further corroborated by Table I, where we report the $J=2$ and 4 photoionization yields. These are little affected by variations in photopredissociation yields.

This same effect reproduces itself in the photopredissociation of the $v=10$ level of the diabatically coupled $^1\Pi_g$ potentials (Fig. 6) and the photoionization yield with this

TABLE I. Photodissociation and photoionization yields for partial waves $J=2$ and 4 as a function of intermediate resonance v, intensities I, and phase ϵ.

v	$I2$ (W/cm^2)	$I4$ (W/cm^2)	ϵ (radian)	Photodissociation $J=2$	Photodissociation $J=4$	Photoionization $J=2$	Photoionization $J=4$
0	7359	5.0E+8	0.37π	6.3E−19	6.8E−16	2.4E−22	2.7E−23
0	7359	5.0E+8	1.37π	1.7E−14	7.4E−16	1.4E−21	3.0E−22
0	3747	5.0E+8	0.54π	1.6E−15	7.1E−16	2.2E−26	8.9E−24
0	3747	5.0E+8	1.54π	9.0E−15	7.0E−16	6.6E−22	1.7E−22
10	16	5.0E+8	1.6π	3.0E−23	2.9E−22	3.6E−24	2.2E−24
10	16	5.0E+8	0.6π	1.1E−19	2.5E−22	6.4E−24	2.6E−24
10	32	5.0E+8	2π	1.1E−19	3.0E−22	8.3E−27	3.9E−25
10	32	5.0E+8	π	1.8E−19	2.2E−22	1.6E−23	5.6E−24

same level as intermediate resonance (Fig. 7). Thus in the former, suppression of dissociation occurs at $\epsilon=1.6\pi$ and $I_2=15.9$ W/cm^2, whereas in the latter, an ionization yield minimum occurs at $\epsilon=1.99\pi$ and $I_2=32$ W/cm^2. The photopredissociation angular distribution evolves again from a $J=2$ partial wave behavior (Fig. 8) to a $J=4$ partial wave angular distribution (Fig. 9) as the $J=2$ component is suppressed at $\epsilon=1.6\pi$. This is in agreement with Table I, where we report the photopredissociation yields for each partial wave. Thus at $\epsilon=0.6\pi$, the $J=2$ dissociation yield is three orders of magnitude larger than that for $J=4$, whereas at $\epsilon=1.6\pi$, the $J=4$ partial wave dominates by one order of magnitude. Similarly, Table I shows the various partial wave contributions to the ionization yield, illustrating once again the independence of both dissociation and ionization processes because of the presence of nonresonant contributions to the latter.

Our results imply that control of ionization and predissociation are independent, whereas Brumer and Shapiro[28] have shown that control should end after the dissociation step. In the present scenario, the independent control of the two processes (ionization vs predissociation) comes from the fact that the $1\,^1\Pi_u \rightarrow 1\,^1\Pi_g$ transition (Fig. 1), is a continuum–continuum transition which is operative and has a large transition moment $\sim R/2$. The continuum $1\,^1\Pi_g$ states now act as intermediate resonance states for the ionization. In previous work, we have shown[15] that the nonresonant amplitude which depends on the principal part PP of $G(\Pi_g)$ [Eqs. (29) and (32)] is often dominant over the resonant contribution [the delta function $\delta(E)$ part of Eq. (32)]. Hence nonresonant amplitudes from intermediate continuum states contribute largely to the ionization process. The photopredissociation process ends at

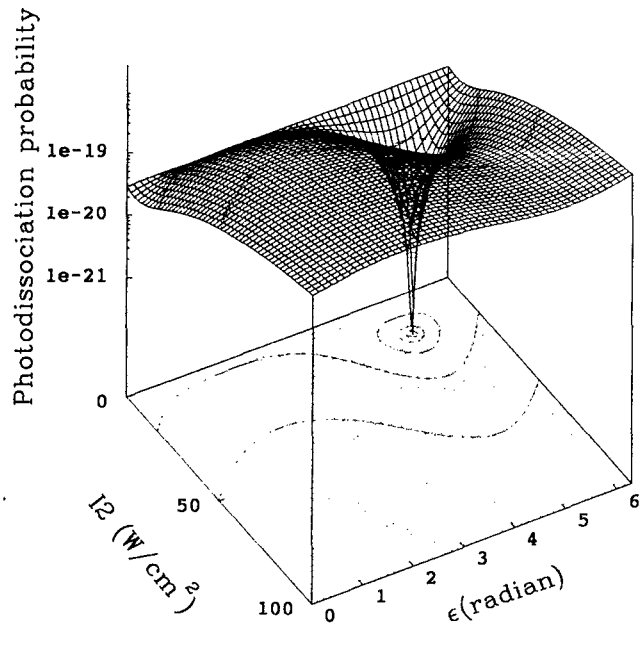

FIG. 6. Photopredissociation probability via the $v=10$, $J=2$ level of the $2\,^1\Pi_g$ state for fixed $I_4=5\times10^8$ W/cm^2 vs I_2 and relative phase ϵ. Minimum occurs at $I_2=15.9$ W/cm^2, $\epsilon=1.6\pi$. $\omega_2=2\omega_4=35\,930$ cm^{-1}.

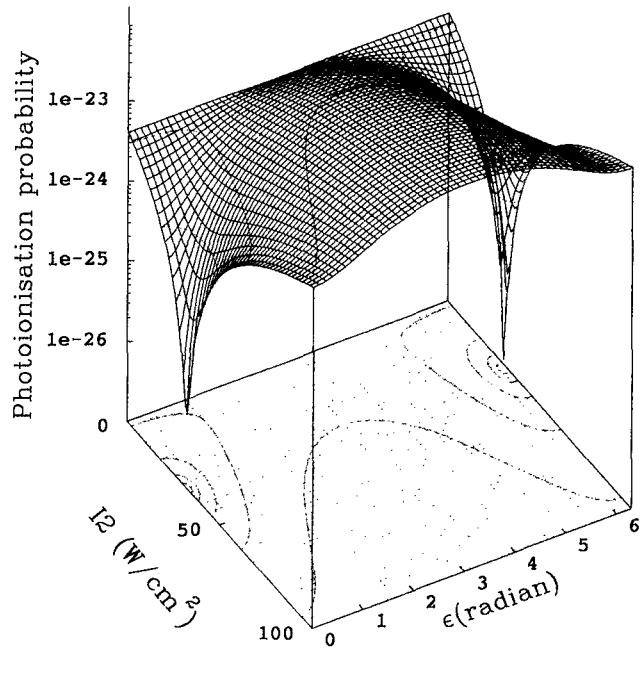

FIG. 7. Photoionization yields in partial wave $J=2$ with the $v=10$, $J=2$ level of $2\,^1\Pi_g$ as intermediate resonance for $I_4=5\times10^{18}$ W/cm^2 vs I_2 and relative phase ϵ. Minima occur at $I_2=32$ W/cm^2 and $\epsilon=0$, 1.99π. $\omega_2=2\omega_4=35\,930$ cm^{-1}.

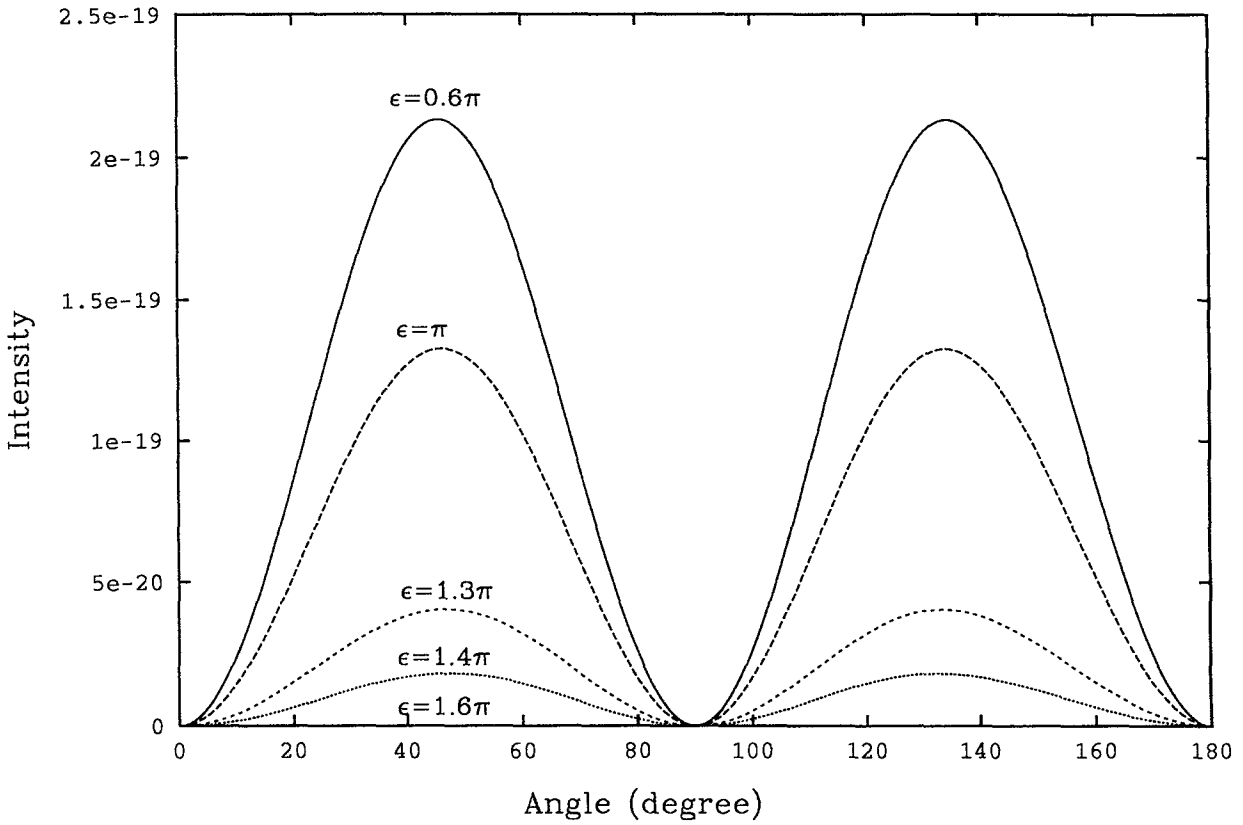

FIG. 8. Photopredissociation angular distribution for $v=10$, $J=2$ level at the minimum of Fig. 6 $I_4=5\times10^8$ W/cm^2, $I_2=15.9$ W/cm^2 vs relative phase ϵ. $\omega_2=2\omega_4=35\,930$ cm^{-1}.

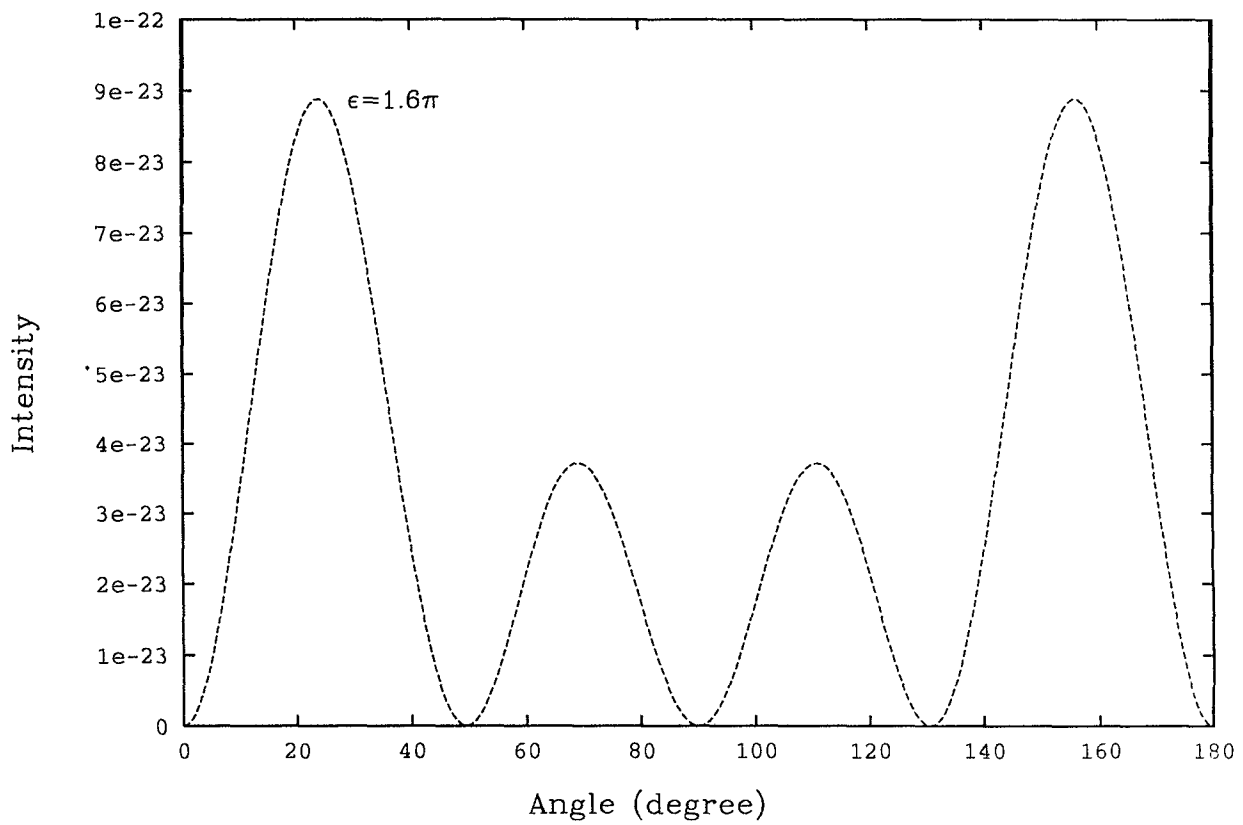

FIG. 9. Photopredissociation angular distribution for $v=10$, $J=2$ at the minimum condition $I_4=5\times10^8$ W/cm^2, $I_2=15.9$ W/cm^2, $\epsilon=1.6\pi$. Distribution is indicative of the $J=4$ partial wave contribution. $\omega_2=2\omega_4=35\,930$ cm^{-1}.

precisely one continuum $1\,^1\Pi_g$ state only, i.e., the resonant state obeying the condition $E(v=0, J=0, X\,^1\Sigma_g^+)+2\hbar\omega_2 = E(k, J=2, 1\,^1\Pi_g)$. This is the same energy which defines the resonant $\delta(E)$ part of the ionization. Clearly, the nonresonant contributions to the ionization are independent of the resonant part, which also controls the photopredissociation amplitude. Finally, from Table I, one concludes that excellent control of either ionization or photopredissociation is only possible provided one partial wave, i.e., J final state, is dominant in either multiphoton process.

ACKNOWLEDGMENTS

We thank CEMAID the national network of Centers of Excellence in Molecular and Intrafacial Dynamics for supporting this research. Contribution from the National Centers of Excellence in Molecular Dynamics.

[1] P. Brumer and M. Shapiro, Chem. Phys. Lett. **126**, 541 (1986); Acc. Chem. Res. **22**, 407 (1989).
[2] M. Shapiro, J. W. Hepburn, and P. Brumer, Chem. Phys. Lett. **149**, 451 (1988).
[3] D. J. Tannor, R. Kosloff, and S. A. Rice, J. Chem. Phys. **85**, 5805 (1986).
[4] S. Chelkowski, A. D. Bandrauk, and P. B. Corkum, Phys. Rev. Lett. **65**, 2355 (1990).
[5] S. Chelkowski and A. D. Bandrauk, Chem. Phys. Lett. **186**, 264 (1991); J. Chem. Phys. **99**, 1185 (1993).
[6] W. Jakubetz, J. Manz, and H. J. Schreier, Chem. Phys. Lett. **165**, 100 (1990).
[7] H. Rabitz and S. Shi, *Advances in Molecular Vibrations and Collision Dynamics* (Academic, New York, 1991), Vol. 1A, p. 187.
[8] A. D. Bandrauk, *Molecules in Laser Fields* (Marcel Dekker, New York, 1993).
[9] C. Chen and D. S. Elliott, Phys. Rev. Lett. **65**, 1727 (1990).
[10] S. Lu, S. M. Park, Y. Xie, and R. J. Gordon, J. Chem. Phys. **96**, 6613 (1992).
[11] A. D. Bandrauk, J. M. Gauthier, and J. F. McCann, Chem. Phys. Lett. **200**, 399 (1992).
[12] S. D. Peyerimhoff and R. J. Buenker, Chem. Phys. **57**, 279 (1981).
[13] F. Grein, S. D. Peyerimhoff, and R. J. Buenker, Can. J. Phys. **62**, 1928 (1984).
[14] L. Li, R. J. Lipert, H. Park, W. A. Chupka, and S. D. Colson, J. Chem. Phys. **88**, 8 (1988).
[15] A. D. Bandrauk and N. Gélinas, J. Chem. Phys. **86**, 5257 (1987).
[16] A. D. Bandrauk and O. Atabek, Adv. Chem. Phys. **73**, 823 (1988).
[17] J. F. McCann and A. D. Bandrauk, Phys. Rev. A **42**, 2806 (1990); J. Chem. Phys. **96**, 903 (1992).
[18] A. D. Bandrauk and M. S. Child, Mol. Phys. **19**, 95 (1970).
[19] H. Lefebvre-Brion and R. W. Field, *Perturbations in Spectra of Diatomic Molecules* (Academic, Orlando, 1986).
[20] S. Miret-Artes, O. Atabek, and A. D. Bandrauk, Phys. Rev. A **45**, 8056 (1992).
[21] D. M. Brink and G. R. Satchler, *Angular Momentum* (Clarendon, Oxford, 1968).
[22] M. Shapiro, J. Chem. Phys. **56**, 2582 (1972).
[23] A. D. Bandrauk and G. Turcotte, J. Chem. Phys. **77**, 3867 (1982).
[24] D. W. Norcross and M. J. Seaton, J. Phys. **36**, 614 (1973).
[25] A. D. Bandrauk, E. Constant, and J. M. Gauthier, J. Phys. II **1**, 1033 (1991).
[26] R. S. Mulliken, J. Chem. Phys. **7**, 20 (1939).
[27] M. Mittleman, *Theory of Laser–Atom Interactions* (Plenum, New York, 1982).
[28] P. Brumer and M. Shapiro, Faraday Discuss. Chem. Soc. **82**, 177 (1986).